Molecular Microbiology (2008) 70(2), 311–322 ■
doi:10.1111/j.1365-2958.2008.06402.x
First published online 27 August 2008

Assembly of the translocase motor onto the preprotein-conducting channel

Spyridoula Karamanou,[1] Vassiliki Bariami,[1,2] Efrosyni Papanikou,[1,2†] Charalampos G. Kalodimos[3] and Anastassios Economou[1,2*]

[1]*Institute of Molecular Biology and Biotechnology-FoRTH, PO Box 1385, Iraklio, Crete, Greece.*

[2]*Department of Biology-University of Crete, PO Box 1385, Iraklio, Crete, Greece.*

[3]*Chemistry and Chemical Biology, Biomedical Engineering, Rutgers University, 599 Taylor Rd, Piscataway, NJ 08854, USA.*

Summary

Bacterial protein secretion is catalysed by the SecYEG protein-conducting channel complexed with the SecA ATPase motor. To gain insight into the SecA–SecYEG interaction we used peptide arrays, thermodynamic quantification, mutagenesis and functional assays. Our data reveal that: (i) SecA binds with low affinity on several, peripheral, exposed SecYEG sites. This largely electrostatic association is modulated by temperature and nucleotides. (ii) Binding sites cluster in five major binding 'regions': three that are exclusively cytoplasmic and two that reach the periplasm. (iii) Both the N-terminal and c-terminal regions of SecA participate in binding interactions and share some sites. (iv) Several of these sites are essential for translocase catalysis. Our data provide residue-level dissection of the SecYEG–SecA interaction. Two models of assembly of SecA on dimeric SecYEG are discussed.

Introduction

Secretion of bacterial preproteins to the periplasm and outer membrane is mediated by the Sec preprotein 'translocase' or 'translocon' (Papanikou *et al*., 2007; Rapoport, 2007). Translocase comprises a transmembrane protein-conducting channel built of three polypeptides SecY, SecE and SecG (hereafter SecYEG) (Fig. 1A) (Brundage *et al*., 1990; Van den Berg *et al*., 2004) and the SecA ATPase (Papanikou *et al*., 2007). SecA bound to SecYEG undergoes nucleotide-driven conformational changes thought to represent 'insertion–deinsertion cycles' (Economou and Wickner, 1994; Economou *et al*., 1995). In several studies, the peripheral SecA was found in integral membrane states (Economou and Wickner, 1994; Kim *et al*., 1994; Economou *et al*., 1995; Chen *et al*., 1996; Eichler and Wickner, 1997) protruding as far as the periplasm (van der Does *et al*., 1996; Ramamurthy and Oliver, 1997; Eichler and Wickner, 1998). These events are apparently coupled (Economou and Wickner, 1994; Economou *et al*., 1995) with segmental preprotein transfer across the membrane through SecYEG (Schiebel *et al*., 1991; Joly and Wickner, 1993).

Individual high-resolution structures of SecYEG (Van den Berg *et al*., 2004) (Fig. 1A) and SecA (see Papanikou *et al*., 2007 and references therein) are available. However, how these subunits assemble to form the functional translocase and which regions of SecYEG associate to SecA remain unknown. Peptide arrays (van der Sluis *et al*., 2006; Robson *et al*., 2007), *in vivo* site-directed cysteine mutagenesis and cross-linking (Mori and Ito, 2006) have revealed possible binding sites but yielded some contradicting results and these sites have not been validated by functional assays. Several mutations that affect SecYEG function have been identified (Matsumoto *et al*., 1997; 2000; van der Wolk *et al*., 1998; Manting *et al*., 1999) but none of these has been demonstrated to directly affect the functional or physical association of SecA with SecYEG. Monomeric (Van den Berg *et al*., 2004) or dimeric (Breyton *et al*., 2002; Mitra *et al*., 2005) SecYEG structures have not revealed any obvious 'cavities' or 'clefts' where SecA could insert and become shielded from phospholipids (Eichler *et al*., 1997; van Voorst *et al*., 1998). Addressing SecA–SecYEG topology is further obscured by controversy concerning the functional quaternary structure of the holoenzyme and its components: SecYEG was seen to form monomers (Yahr and Wickner, 2000; Van den Berg *et al*., 2004), 'back to back' (Breyton *et al*., 2002) or 'front to front' (Mitra *et al*., 2005) dimers and tetramers (Manting *et al*., 2000; Scheuring *et al*., 2005). Moreover, SecA forms monomers (Or *et al*., 2002; Duong, 2003) or dimers (de Keyzer *et al*.,

Accepted 4 August, 2008. *For correspondence. E-mail aeconomo@imbb.forth.gr; Tel. (+30) 2810 391166; Fax (+30) 2810 391166. †Present address: Department of Molecular Genetics and Cell Biology, The University of Chicago, 920 East 58th Street, CLSC 801, Chicago, IL 60637, USA.

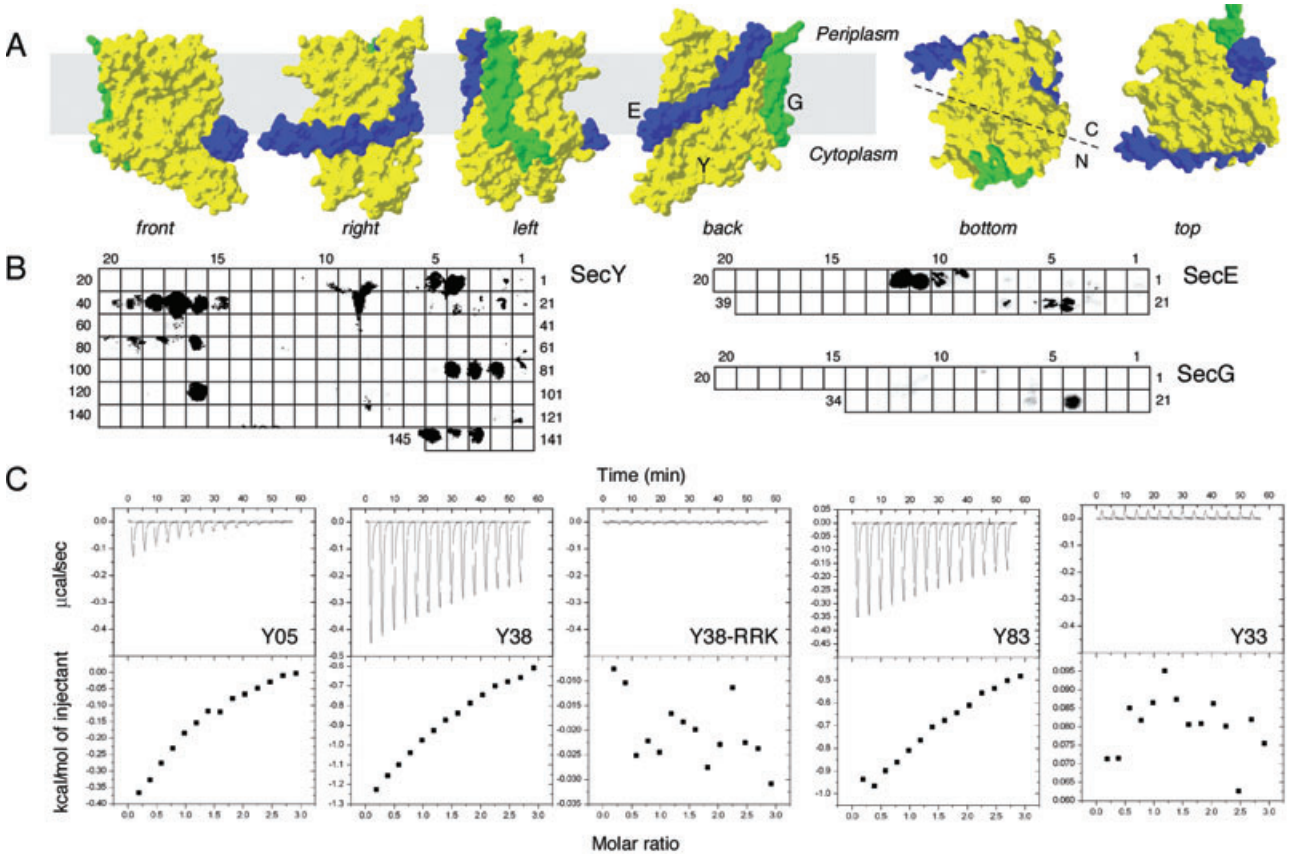

Fig. 1. Binding of SecA to SecYEG peptides.
A. Surface representation of a model of the *E. coli* SecYEG structure derived from the original structure of SecYEG from *M. jannaschii* (Van den Berg *et al*., 2004). SecY (yellow) has 10 transmembrane (TM) helices and its 'lateral gate' exposed in the 'front' view. The 10 TM of SecY can be split into two symmetrical halfs (N and C; see 'bottom' view). *ec*SecE (blue) contains three helices but only two helices are present in the *mj*SecYEG complex and these embrace the flexible SecY structure. SecG (green) is almost perpendicular to the plane of the membrane. Structures were visualized with SwissPDBViewer.
B. Binding of SecA to a SecYEG peptide array.
A representative experiment (as described in *Experimental procedures*) of SecA binding to the SecYEG peptide array at 4°C, immunostained with an α-SecA antibody (1:100 000 dilution).
C. Binding of SecY peptides to SecA in solution. 13mer soluble peptides corresponding to some of the immobilized peptides in the array were synthesized and tested by ITC for binding to SecA.

2005; Jilaveanu *et al*., 2005), combinations of monomers or dimers interacting with SecYEG monomers (Tziatzios *et al*., 2004) or tetramers (Manting *et al*., 2000; Scheuring *et al*., 2005). Atomic resolution structures of the SecA–SecYEG holoenzyme that could resolve some of these issues are not yet available.

To investigate SecA–SecYEG assembly *ab initio* without assuming any prior knowledge we used an immobilized peptide array covering the full length of all SecYEG components. Binding was subsequently validated through a combination of quantitative biophysical measurements, mutagenesis and functional assays. This approach identified peripheral regions on SecYEG that interact with SecA, forming a multivalent receptor with several low-affinity sites. Several of these are essential for catalysis. Binding is electrostatic and involves predominantly cytoplasmic loops and minor membrane-embedded sites. Both SecA structural domains contribute to binding. SecA–SecYEG association is dynamic and regulated by temperature and nucleotides.

Results

SecYEG peptides that bind SecA

To determine SecYEG segments that interact with SecA we used arrays of 13 residue-long peptides that spanned the entire length of the three polypeptides [Table S1; Y01–Y145 (SecY); E01–E39 (SecE); G01–G34 (SecG)]. Purified SecA was incubated with the array at 4°C. SecA that remained bound on the immobilized peptides after extensive washes was blotted onto a polyvinylidene difluoride (PVDF) membrane and immunostained with an α-SecA antiserum (Karamanou *et al*., 1999). Binding profiles that

were reproducible in three to five repeat experiments (e.g. see Fig. 1B) and were above certain thresholds (see legend to Table S2) were analysed further. A few SecYEG peptides bind SecA. These are distributed in five 'regions' along the primary sequence (Fig. 2, α–ε; see below).

The most prominent signals seen were with: SecY peptides (Y04 and Y05, Y35–40, Y76–78, Y82–84, Y116, Y121–122 and Y143–145); SecE (E11–12 and E24–25) and SecG (G24). Only Y76 contains hydrophobic residues from one of the 14 transmembrane helices of SecYEG. In most cases SecA bound to a number of overlapping peptides. Thus minimal binding sites could be delimited (Table S2). The apparent binding strength per aminoacyl residue in each peptide was estimated using different antiserum dilutions (Fig. 2A and Table S2).

Quantification of SecA binding to SecYEG peptides

To scrutinize the array data and quantify binding, three peptides displaying the strongest binding (Y05, Y38, Y83) were chemically synthesized and their binding to SecA was measured using isothermal titration calorimetry (ITC) (Fig. 1C). Three peptides that do not bind SecA in the array (Y33, Y87, Y112) were used as 'controls'. If measurable enthalpy changes occur during a bimolecular interaction ITC can measure them as well as determine the dissociation constant (K_D) and the stoichiometries of the complexes. Y05, Y38 and Y83 show significant enthalpy changes and therefore clearly associate with SecA in solution. Complexes display ~1:1 stoichiometries and occur with low affinities of 27–280 μM. Alanyl substitution of $R_{113}R_{114}K_{115}$ in Y38 abolished ITC-detectable binding (Fig. 1C; see 'Y38-RKK'). Control peptides showed no detectable binding by ITC (e.g. Y33; Fig. 1C; Y87 and Y112 are not shown).

Clearly, ITC corroborates that SecYEG peptides identified by the peptide array bind to SecA. These data provide the first demonstration of direct SecA binding to defined, extremely short segments of the protein-conducting channel.

Mapping of SecA docking sites on the three-dimensional structure of SecYEG

We next mapped the sites of SecYEG recognized by SecA (Fig. 2A; Greek letters) onto a secondary (Fig. 2G) and a tertiary surface (Fig. 2H) model of the *Escherichia coli* SecYEG derived from the homologous *Methanocaldococcus jannaschii* structure (Van den Berg *et al*., 2004). Practically all of these residues are located in the periphery of SecYEG and their side-chains are exposed and available for possible external interactions. With the exception of two minor sites (γ_1 and β_{1-3} in the periplasmic face of SecYEG), all the binding occurs at cytoplasmic regions of SecY and SecE. Interestingly, such peptides might not be continuous in the primary sequence of a polypeptide yet they assemble in three-dimensional space so as to form composite continuous binding surfaces that we term 'regions' (e.g. δ and ε). Peptides of region β and γ fall on the same side of SecYEG but are otherwise dispersed on the primary sequences. Sites ε_1 and ε_2 derive from the N-terminal (TM1–5) and C-terminal (TM6–10) half of SecY, respectively, but are proximal in three-dimensional space (see Fig. 2H, 'bottom' view). Three regions formed by six cytoplasmic binding sites are the most prominent binders: α_1, $\delta_1+\delta_2+\delta_3$ and $\varepsilon_1+\varepsilon_2$. Another major site in SecE (aa 30–40) is predicted to be cytoplasmic but cannot be mapped as this region is absent from the *mj*SecE structure.

The cytoplasmic face of SecY contains a preponderance of charged residues (Fig. 3A). It is therefore not surprising that in almost all of the sites identified here, charged residues are present (Table S2) and important for SecA binding (Fig. 1C, 'Y38-RRK'). Binding of SecA to SecYEG is abrogated when 0.3 M KCl is added, as determined by a membrane flotation assay (Fig. 3I). Apparently, SecA–SecYEG assembly is driven by a strong electrostatic component.

SecA–SecYEG interaction is modulated by temperature and nucleotides

Nucleotides and temperature control translocase catalysis (Sianidis *et al*., 2001; Hunt *et al*., 2002; Schmidt *et al*., 2000). Do they also regulate SecA–SecYEG assembly? To test this binding of SecA at 4°C or 37°C in the presence of ADP or the non-hydrolysable ATP analogue AMP-PNP was examined (Fig. S1). Results were quantified and mapped onto the primary sequences (Fig. 2).

At 4°C, addition of nucleotide causes only minor differences in the profile or strength of peptide binding (compare Fig. 2B and C with Fig. 2A). However, at 37°C the observed SecA binding footprint on SecYEG was altered in some regions (compare Fig. 2D with Fig. 2A). This included the appearance of new binding sites (e.g. γ_3), the disappearance of others that were prominent at 4°C (e.g. δ_2/δ_3) or the shifting of others in the SecYEG primary sequence (Fig. 2B; Table S2). In general, at 37°C binding occurred to SecYEG sequences that are more hydrophobic and integral to the membrane. ADP addition led to a pattern that closely resembles that seen at 4°C (compare Fig. 2E with Fig. 2B). The AMP-PNP-derived pattern at 37°C (Fig. 2F) was intermediate to that of the two previous states.

Collectively, our data demonstrate that SecA can bind to SecYEG as an apoprotein. Nucleotides and temperature can modulate SecA association with certain sites of its polyvalent SecYEG receptor. These dynamic interactions

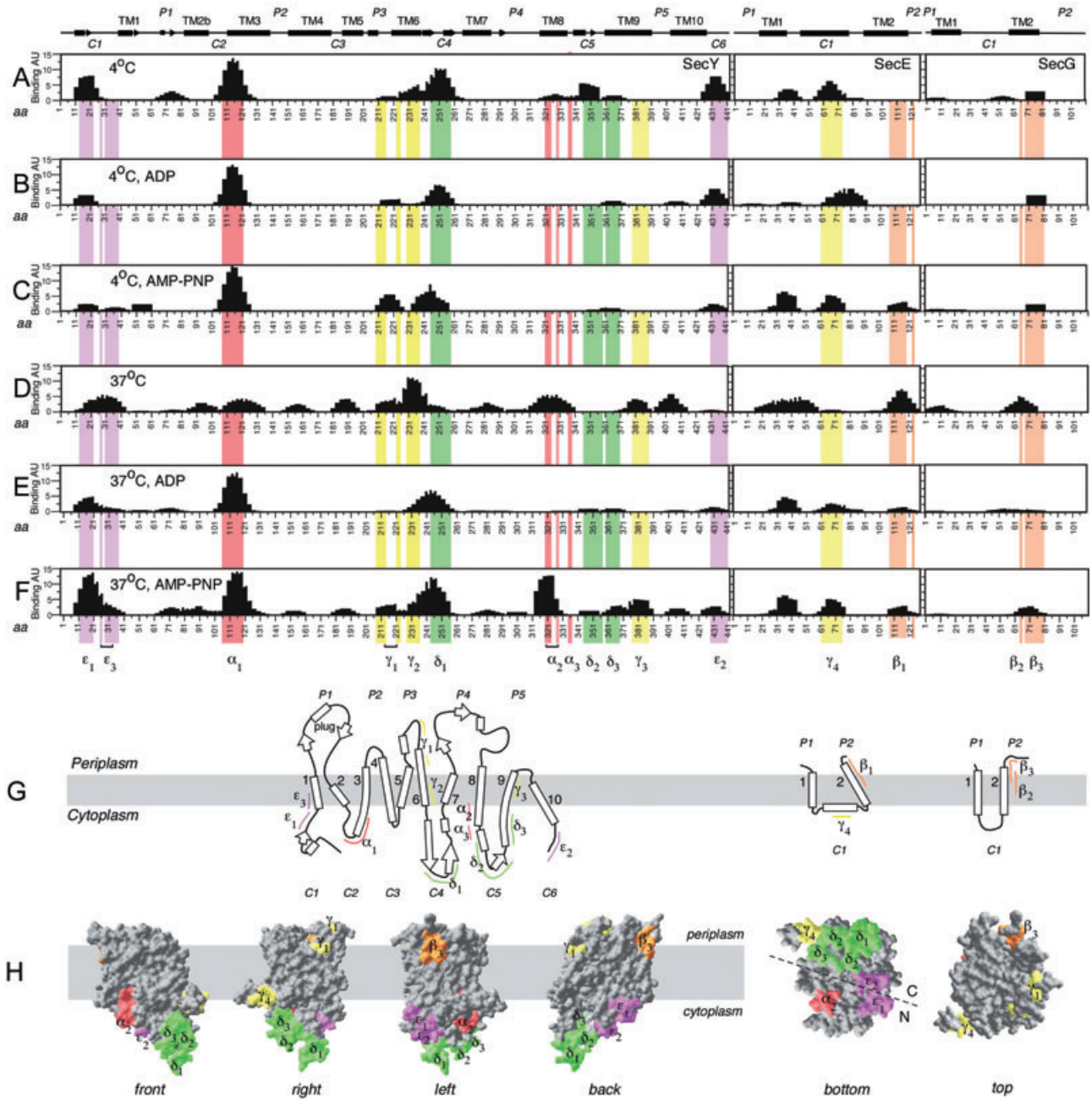

Fig. 2. Quantification of binding strength and mapping of the SecA binding regions of SecYEG.
A–F. SecY regions that bind SecA are indicated with residue-level resolution on a linear map of the primary sequence of SecY, SecE and SecG. To facilitate localization of the sites the secondary structure of the proteins is shown at the top including their transmembrane regions (TM), cytoplasmic (C) and periplasmic (P) loops. TM2b is also known as the 'plug' substructure that folds into the channel or can flip out. The height of the bars in the graph indicates apparent 'Binding Strength' expressed in Arbitrary Units. SecA (100 nM) was incubated with the peptide array at the indicated temperature and nucleotide regimes. The Greek letters denote the five distinct binding regions and the numbers in subscript their subsites. The coloured bars highlight the binding regions in the six graphs and are: red (α), orange (β); yellow (γ); green (δ); and magenta (ε).
G. The secondary structure elements of SecYEG (as in the top of this figure) were assembled in a two-dimensional transmembrane spanning model derived from the determined structure (Van den Berg *et al*., 2004). TMs are denoted here with numbers. The binding sites determined in (A)– (F) are shown here as coloured lines with their Greek alphanumerical labels below.
H. Data from (A)–(F) were mapped on a surface model of SecYEG identical to that in Fig. 1A. SecYEG are shown here in grey and only the SecA binding sites are coloured.

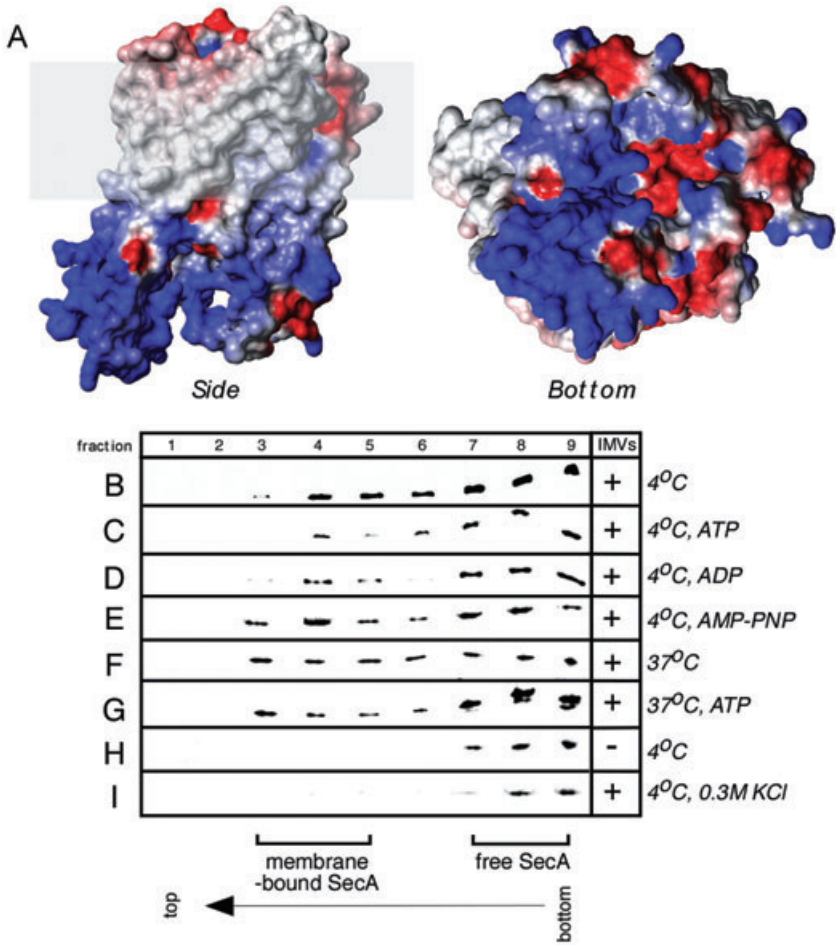

Fig. 3. Binding of SecA to SecYEG-containing membranes by flotation analysis.
A. The electrostatic potential of SecY was determined using the GRASP algorithm. Positive charges are blue and negative charges are red. The grey band in the side view represents non-polar/hydrophobic residues forming the hydrophobic core of the membrane plane.
B–I. SecA binding to SecYEG-containing inverted inner membrane vesicles (IMVs). A flotation gradient centrifugation assay was used (Beck *et al*., 2000; Karamanou *et al*., 2005; Papanikou *et al*., 2005) and bound SecA was visualized by immunostaining with α-SecA antibodies. IMVs float inside the gradient in fractions 3–5 (Karamanou *et al*., 2007). SecA alone (H) sediments to the bottom of the gradient (fractions 7–9) while SecA bound to IMVs floats to fractions 3–5 (B–G).

cannot be dissected with methods assaying for SecA binding overall to membrane-embedded SecYEG (Fig. 3C–G) (Natale *et al*., 2004).

Binding of SecA domains onto SecYEG

To identify SecA regions that interact with SecYEG we employed truncated SecA derivatives (Fig. 4; Fig. S2). SecA(9–834) is a fully functional, dimeric SecA that is missing the N-terminal nonapeptide and the C-tail (Karamanou *et al*., 2005; Gelis *et al*., 2007); SecAΔC is missing the C-terminal domain of SecA (Karamanou *et al*., 1999; Vrontou *et al*., 2004); the C34 polypeptide encompasses the C-domain of SecA. SecA(9–834) binds to all of the sites determined for wild-type SecA (compare Fig. 4A with Fig. 2A) with the exception of very weak binding to ε_1 and δ_3 and no detectable binding to $\alpha_{2/3}$, δ_2, $\varepsilon_{2/3}$ and $\beta_{2/3}$. Reproducible binding is seen with either C34 (Fig. 4B) or SecAΔC (Fig. 4C) indicating that both regions of SecA bind to SecYEG. Remarkably, despite some obvious shifts in the binding frame (e.g. compare $\varepsilon_{1/3}$ and α_1 in Fig. 4B and C), most of the main cytoplasmic binding regions appear to be used by both SecA substructures.

We next examined whether ADP or/and temperature affect the binding of SecAΔC to SecYEG (Fig. 4C–F). SecAΔC not only retains many of the binding characteristics of the complete SecA but also its binding appears to be similarly regulated by temperature and nucleotide. Binding of C34 could not be detected at 37°C (not shown) suggesting a weaker or more transient interaction with SecYEG at elevated temperature.

Mutations in SecA binding sites abrogate SecY function in vivo

To validate the functional importance of the identified SecA binding sites we used alanine mutagenesis (see *Experimental procedures* and *Supporting information*). Mutations were generated on pET610, a plasmid carrying a recombinant *secYEG* operon (van der Does *et al*., 1998). To exclude the possibility of indirect effects caused by the mutations (e.g. instability, reduced membrane insertion, etc.) the amount of SecY in the membranes of all mutants was determined by immunostaining (data not shown). Twenty-one SecY mutant derivatives that were produced to wild-type levels were studied further (Table S3).

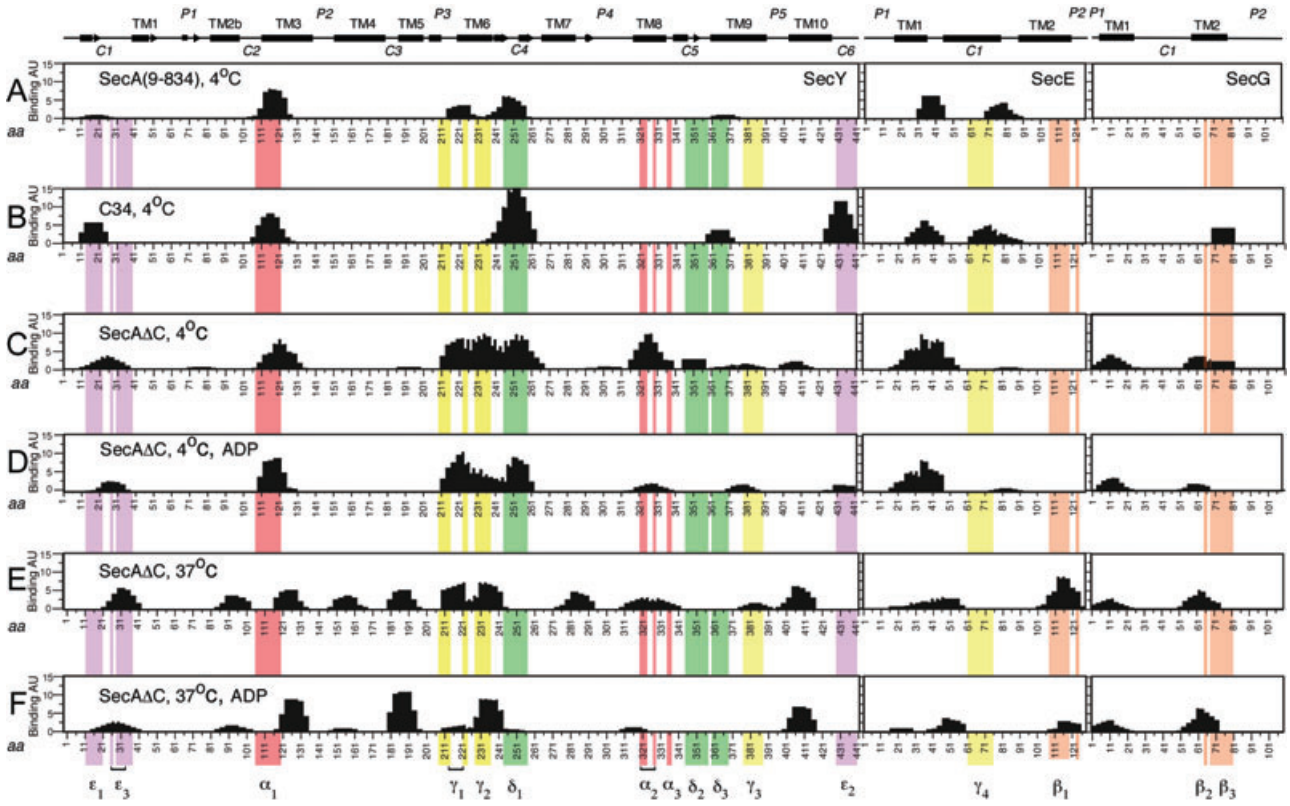

Fig. 4. Binding of SecA regions to SecYEG. SecY regions involved in binding SecA are colour-coded as in Fig. 2A– F. C34 (aa 609–901) and SecAΔC (aa 1–609) were produced as independent polypeptides (Karamanou *et al.*, 1999).

pET610 restores growth of AF659, an *E. coli* strain harbouring a cold-sensitive *secY* mutation (Baba *et al.*, 1990; Smith *et al.*, 2005), at 20°C, while the vector alone cannot. Sixteen SecY derivatives (Classes I–III) displayed measurable defects in complementation. The location of the most severe mutants is shown in Fig. 5A. Six more mutants (Class IV) with no measurable defects were not studied further. Representative mutants are shown in Fig. 5B (for a complete listing see Table S3). In an *in vivo* assay that monitors secretion of the periplasmic protein alkaline phosphatase mutants of Classes I (Fig. 5C, lane 3) and II (lane 4) were severely defective. Even a Class III mutant (lane 5) shows reduced secretion when compared with wild-type SecY (lane 2).

These data demonstrated that several of the SecY regions identified using the peptide array analysis are important for function *in vivo* and for cell viability.

SecA binding sites on SecY are essential for translocase catalysis

Is the *in vivo* defect of the SecY mutants attributable to compromised SecA-driven protein translocation? To this end, we analysed the *in vitro* translocation of the model preprotein substrate proOmpA into inner membrane vesicles (IMVs) containing wild-type SecYEG or mutant derivatives (Fig. 5D). Class III SecY mutants (e.g. M2, lane 8) retained some, albeit reduced, translocation activity compared with wild-type SecY (lane 3), while no proOmpA translocation was detected with Class I or II mutants (e.g. M15 and M4; lanes 6 and 7) or with the uncomplemented *secYcs* strain (lane 5). Clearly, the SecY mutants severely compromise SecA-dependent protein translocation. This defect was not corrected by provision of proton motive force (data not shown).

Additionally, we examined the ability of SecY mutants to stimulate SecA basal ATPase at 37°C (Fig. 5E) or 20°C (Fig. S3A). In this assay, basal SecA ATPase is significantly stimulated upon addition of wild-type SecYEG-containing IMVs (membrane ATPase; lane 2) or IMVs plus proOmpA (translocation ATPase; lane 3). All SecY mutant derivatives (lanes 6–17) or the uncompleted *secYcs* strain (lanes 4 and 5) fail to stimulate SecA basal ATPase at either temperature. Reduced membrane ATPase activity is suggestive of compromised interaction with SecYEG that could lead to suboptimal priming (Papanikou *et al.*, 2007). This defect was further quantified by using a range of IMV concentrations for wild-type and three representa-

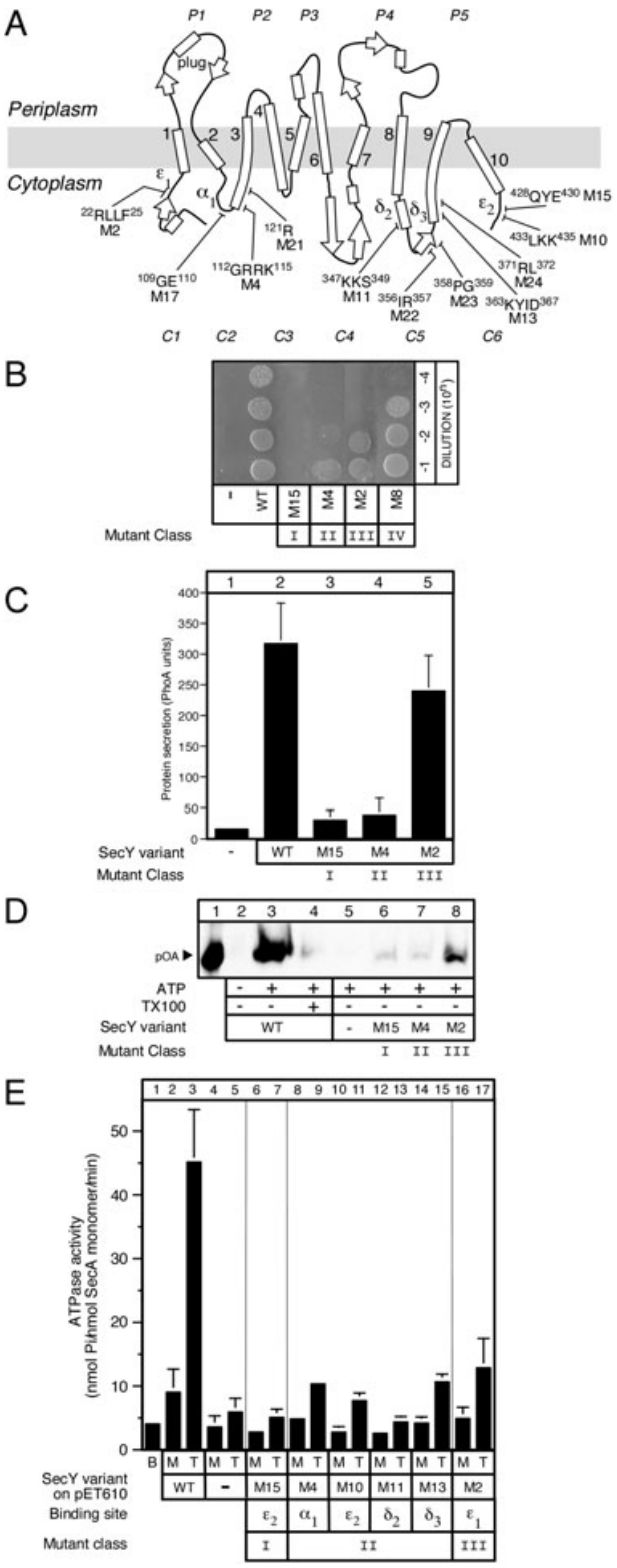

Fig. 5. Functional analysis of the SecA binding regions of SecY.
A. Map of mutations generated in this study and that display the strongest defects. The location of 11 of the mutations generated and the residues affected are indicated. For a complete list of the 21 mutations see Table S3.
B. *In vivo* genetic complementation analysis. Genetic complementation test, at 20°C, of the AF659 *secYcs* strain (Baba *et al*., 1990; Taura *et al*., 1994). The strain was transformed with a vector carrying *secY* or *secY* mutants or with no insert as a control. AF659 *secYcs* transformants were cultured at 37°C until mid-log phase. Cells were serially diluted with LB and 6 µl of each was spotted on LB agar plates, which were photographed after 72 h at 20°C. Only four representative mutants are shown here. All strains grew fully at the permissive temperature of 37°C (not shown).
C. Protein translocation *in vivo*. Plasmids encoding wild-type SecY or mutants M2, M4, M15 under the control of the *ptrc* promoter were introduced into *E. coli* strain JM109 (DE3) along with pBAD22 derivative plasmids encoding wild-type proPhoA under the control of the *ara* regulon. The cells were grown at 37°C until $OD_{595} = 0.2$. SecYEG synthesis was induced with 0.2 mM IPTG and phosphatase activity was measured at 414 nm using *p*-nitrophenol phosphate as a substrate. Activity units are defined as $(OD_{414} \times 1000)/(OD_{595} \times$ incubation time) (Derman *et al*., 1993). Background values from chromosomal SecYEG were determined in the same experiment and subtracted from the corresponding values of plasmid-expressed SecYEG. Error bars represent the standard deviation from measurements of three independent cultures each in triplicate.
D. *In vitro* protein translocation. *In vitro* protein translocation of SecY and representative SecY derivatives. ATP-driven translocation of proOmpA-His (0.1 mg ml^{-1}) into inverted inner membrane vesicles (IMVs) carrying mutated derivatives of SecY [14 µg of SecY; 100 µl of reactions in buffer B, BSA (0.5 mg ml^{-1}), 1 mM ATP, 1 mM DTT and SecB (0.04 mg ml^{-1})] catalysed by SecA. Samples were incubated at 37°C for 15 min and reactions were stopped at 4°C followed by addition of proteinase K (1 mg ml^{-1}; 10 min; 4°C). Proteins were precipitated with trichloroacetic acid (TCA; 15% w/v), analysed by SDS-PAGE and immunostained with α-His antibody. Lane 1: 10% of undigested proOmpA-His input. Lane 4: membranes were dissolved with Triton X-100 (1% v/v) before proteinase K addition.
E. *In vitro* translocation ATPase assays. The K_{cat} values [pmol Pi (pmol SecA protomer)$^{-1}$ min^{-1}] of basal, membrane (urea-treated IMVs; 17 µg of protein ml^{-1}) and translocation (IMVs plus 60 µg ml^{-1} proOmpA) ATPase activities of SecY and of its indicated derivatives were determined at 37°C. To exclude background values from the small amounts of the chromosomally encoded SecY, IMVs prepared from strain AF569 carrying the vector alone were also prepared. Values for these IMVs were determined in the same experiment and were subtracted from the corresponding values of the IMVs harbouring mutant SecYs.

tive SecY mutants (Fig. S3B). Increasing the amount of added IMVs leads to an eightfold stimulation of SecA ATPase activity when wild-type SecY is used, while little or no stimulation is seen with the mutant IMVs.

We concluded that the SecY regions identified here are essential for a functional SecA–SecY interaction and subsequent SecA-mediated protein translocation.

SecA binding sites on SecY are essential for functional activation of SecA

Individually mutated sites of a polyvalent, discontinuous receptor would be expected to reduce the overall affinity of SecA for SecYEG. To test this hypothesis we quantified the affinity of [^{35}S]-SecA for IMVs carrying mutant SecY derivatives as described (Hartl *et al*., 1990; Vrontou *et al*., 2004) (Table 1; Fig. S4). Indeed, the affinity of SecA for IMVs containing Class I and II SecY mutants is reduced

Table 1. Equilibrium dissociation constants of [^{35}S]-SecA binding to inverted inner membrane vesicles harbouring SecY and mutated derivatives were determined as described (Vrontou *et al.*, 2004).

SecY	K_D
Wild type	62 (±10)
M15-(^{428}QYE^{430})	310 (±43)
M4-(^{112}GRRK^{115})	155 (±17)
M2-(^{22}RLLF^{25})	160 (±29)

three- to fivefold. Therefore, the SecY regions identified here are required for efficient SecA–SecYEG assembly.

Discussion

We present the footprint of SecA binding to SecYEG. SecA associates almost exclusively with the charged cytoplasmic face of SecYEG forming several interactions (Fig. 2). Five 'composite' SecYEG regions interact with the large SecA molecule (Fig. 2A–F and Table S2). Each of these interactions is of low affinity (Fig. 1C). Presumably, concomitant binding of SecA to multiple regions results in the high-affinity SecA–SecYEG complex (Hartl *et al.*, 1990). Such poly valent binding is typical when high- and low-affinity states interchange in highly dynamic systems. This property could be critical for the flexible translocase.

SecA binds to SecYEG largely at cytoplasmic regions. Some of the sites identified here agree with partial peptide arrays (Robson *et al.*, 2007) and engineered cysteine cross-linking (Mori and Ito, 2006). Other sites localize on SecYEG residues that are near the *trans* side of the membrane and lie outside the preprotein channel. Such sites would be consistent with periplasmic exposure of SecA regions (den Blaauwen *et al.*, 1997a; Ramamurthy and Oliver, 1997; Eichler and Wickner, 1998) and inserted intermediates. Alternatively, SecG could also interact with SecA at the *cis* side through regions such as β_2/β_3 after invertion of its membrane topology (Nishiyama *et al.*, 1996).

Mutational analysis validated the importance of the SecA binding surfaces on SecY. Several of the mutations we generated result in strong functional defects *in vivo* (Fig. 5B and C) and *in vitro* (Fig. 5D and E; Fig. S3A). Previous studies have also identified mutations in some of the binding sites identified here (Mori and Ito, 2001; Chiba *et al.*, 2002; Smith *et al.*, 2005; Tam *et al.*, 2005). Some of the mutations cause a measurable reduction (up to fivefold) in binding affinity (Table 1; Fig. S4), consistent with a role of the identified sites in SecA binding to SecY. This reduction is rather strong considering the multiplicity of the binding sites and the fact that their individual affinities for SecA are very low. We entertain two possibilities: contribution to SecA binding from the various sites is highly synergistic or, alternatively, minor conformational effects caused by the mutations might misalign the three-dimensional orientation of the multiple weak binding sites.

Importantly, the various sites are not equally involved in binding under all regimes. Thus, three of the binding sites (ε_1, $\alpha_{2/3}$ and δ_1) are used prominently by SecA under all conditions tested and would appear to be more 'static' anchors. The presence of such sites was anticipated as SecA binding to SecYEG does not require nucleotide or elevated temperature (Natale *et al.*, 2004) (Fig. 3B–G). All of the other observed interactions appear to be more 'dynamic' and vary in intensity depending on the experimental conditions. Nucleotides and temperature affect not only SecA conformation (den Blaauwen *et al.*, 1996; Sianidis *et al.*, 2001; Hunt *et al.*, 2002; Keramisanou *et al.*, 2006) but also the strength of SecA binding to some SecYEG sites. For example, binding of SecA at ε_1 is stronger in the AMP-PNP state at physiological temperature (Fig. 2F), while nucleotides abolish binding at δ_2 at 4°C (Fig. 2B and C). ADP binding promotes a more compact SecA state (den Blaauwen *et al.*, 1996; Sianidis *et al.*, 2001; Hunt *et al.*, 2002; Keramisanou *et al.*, 2006) and this state is clearly less prone to hydrophobic interactions seen at 37°C (Fig. 2D). Some of these interactions (e.g. δ_2, ε_2, $\beta_{2/3}$) (Fig. 4A) are susceptible to removal of extreme SecA regions such as the flexible, membrane-inserting C-tail (den Blaauwen *et al.*, 1997a). The C-tail also controls SecA binding to preproteins (Gelis *et al.*, 2007) and SecB (Breukink *et al.*, 1995; den Blaauwen *et al.*, 1997b; Randall *et al.*, 2005).

The C-domain binds prominently to SecYEG at 4°C (Fig. 4B) but loses its binding at physiological temperature (not shown). Previous experiments failed to demonstrate binding of the isolated C-domain to SecYEG (Karamanou *et al.*, 1999; Dapic and Oliver, 2000). These data, together with the observation that the C-domain is particularly flexible (Song and Kim, 1997) and loses its structure at elevated temperature (I. Gelis and C.G. Kalodimos, unpubl. results), suggest that its interaction with SecY is dynamic.

Binding to SecYEG is the result of defined associations from both the N-terminal and the C-terminal regions of SecA (Fig. 4). These data corroborate previous observations that both the C-domain region (Economou and Wickner, 1994; Economou *et al.*, 1995) and the N-terminal region (Eichler and Wickner, 1997; Ramamurthy and Oliver, 1997; Vrontou *et al.*, 2004; Osborne and Rapoport, 2007) can interact with SecYEG. Some of the binding sites appear to be specific for the N-terminal region (e.g. α_1, γ_1, γ_2, δ_2) or the C-domain (ε_1, γ_4, δ_3). Remarkably, however, several of the binding sites on SecYEG share common residues between the C-domain and the N-terminal region of SecA (although differences in the degree of binding and the exact frame are apparent, e.g. compare binding to ε_2 in Fig. 4B and D). We think this

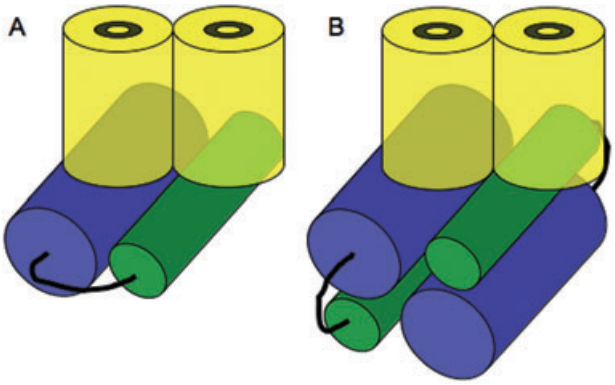

Fig. 6. Working models of SecA interaction to SecYEG. The models take into account data presented here and those from others (Mori and Ito, 2006; Osborne and Rapoport, 2007) with either a monomeric (A) or a dimeric 'head-to-tail' dimer (B) SecA binding to a dimeric SecYEG (yellow cylinders). SecA is depicted as an N-terminal domain (blue) binding to a C-terminal domain (green).

might be due to the quaternary organization of SecYEG that is widely thought to function as a dimer (Bessonneau *et al*., 2002; Tziatzios *et al*., 2004; Osborne and Rapoport, 2007) and to the limited number (six) of cytoplasmic loops available for binding. The model of division of labour in the SecYEG dimer with one SecYEG functioning as a docking station for a single SecA and the other as a preprotein-conducting channel (Osborne and Rapoport, 2007) would be in good agreement with our data (Fig. 6A). Peptide array experiments cannot deconvolute the potential contributions from different SecYEG trimers. Alternative possibilities of a 'head-to-tail' SecA dimer docking on two SecYEG trimers (Fig. 6B) would also be compatible with independent C-domain and N-terminal region binding to a SecYEG dimer. However, we observed identical binding with either monomeric or dimeric SecA (not shown).

In summary, we hypothesize that SecA makes use of both stable docking sites and numerous dynamic sites on the SecYEG dimer as it undergoes nucleotide- and preprotein-driven conformational changes during the translocation reaction. This allows SecA to remain constantly attached to SecYEG, probably with its N-terminal domain, while at the same time undergoing nucleotide-driven conformational changes that affect its business end, i.e. the two specificity domains. These interactions modulate the conformation of the protein-conducting channel and may push or guide segments of the preprotein across the membrane.

Experimental procedures

Strains and plasmids

AF659, a derivative of *E. coli* strain MC4100, carries the SecY39 mutation (R357H) that renders the cells cold-sensitive (Baba *et al*., 1990; Smith *et al*., 2005). For construction of mutant SecY proteins see *Supporting information*.

Binding of SecA to peptide arrays

Peptide arrays were prepared by automated spot synthesis (Jerini Peptide Technologies GmbH) (Reineke *et al*., 2001). Peptides were C-terminally attached to cellulose via a β-Ala spacer. Peptides were derived from protein sequences of *E. coli* SecY (1–145), secE (1–39) and secG (1–34). Each spot carries 5 nmol of peptide covalently bound to the cellulose PEG membrane. Before screening, the dry membrane was washed in methanol (10 min), in high-salt buffer (50 mM Trizma base pH 8, 6.4 mM KCl, 170 mM NaCl) at room temperature (3 × 5 min), in buffer B (50 mM Trizma-base pH 8.0, 50 mM KCl, 5 mM $MgCl_2$) at the desired temperature (5 × 5 min) and finally in equilibration buffer (buffer B, 5 g of sucrose, 100 μg ml^{-1} BSA, 2 mM DTT, 0.01% Tween-20) (15 min).

SecA (100 nM) and SecA domains (200 nM) were allowed to react with the peptide array membrane for 1 h at 4°C or 15 min at 37°C respectively. Free SecA was removed with extended buffer B washes while SecA bound to peptides was electrotransferred onto PVDF membranes (Millipore). PVDF membranes were sandwiched between blotting papers soaked with cathode buffer (25 mM Trizma base, 40 mM aminocaproic, 20% methanol, 0.01% SDS, pH 9.2) and anode buffers ABI, ABII (ABI = 30 mM Trizma-base, 20% methanol, pH 10.5, ABII = 300 mM Trizma-base, 20% methanol, pH 10.5). Bound SecA was detected by α-SecA-specific polyclonal rabbit sera and enhanced chemiluminesence measurement (Pierce) using a fluoroimaging system (Fujifilm; LAS 3000). In order to account for lower-affinity protein–protein interactions a range of dilutions of SecA antisera were used (1:100 000–1:8000). 'Binding Strength' of SecA on each spot was determined as described in Table S2.

ATP hydrolysis measurements

All assays were in buffer B (50 mM Tris-Cl, pH 8, 50 mM KCl, 5 mM $MgCl_2$, 1 mM DTT, 1 mg ml^{-1} BSA and 1 mM ATP). SecA was added at 0.1 mg ml^{-1}. For membrane ATPase IMVs containing SecY or SecY derivatives were added at 1.5 μg of SecY as determined by quantitative Western blots using purified SecY as a marker. For translocation ATPase proOmpA was further added at 20 μg ml^{-1}. Released phosphate and K_{cat} values were measured as described (Karamanou *et al*., 1999; Sianidis *et al*., 2001).

SecA binding to membrane-embedded SecYEG

Binding of [^{35}S]-labelled SecA to IMVs was performed as described elsewhere (Hartl *et al*., 1990). Briefly, urea-treated IMVs (64 μg of membrane protein ml^{-1}) were mixed with a range of [^{35}S]-SecA concentrations (0.5–2000 nM; buffer B; 1 mg ml^{-1} BSA; 15 min; 4°C). Reactions were overlaid on equal volume of buffer B, 0.2 M sucrose, 1 mg ml^{-1} BSA, in centrifuge tubes pre-adsorbed with BSA and sedimented (320 000 *g*; 30 min; 4°C; Beckman TLX120 ultracentrifuge). Pellets, rinsed (twice; 100 μl of buffer B) and re-suspended

by sonication, were spotted on nylon membranes in a vacuum manifold (Bio-Rad). Bound radioactivity was quantified by phosphorimaging (Storm 840; GE Healthcare). Data were fitted to hyberbolae using non-linear regression in Prism (GraphPad). Binding using the flotation assay was as previously described (Papanikou *et al*., 2004).

SecA binding to SecYEG-containing IMVs was also studied suing a flotation gradient centrifugation assay (Beck *et al*., 2000; Karamanou *et al*., 2005; Papanikou *et al*., 2005). Binding of SecA (1 μg) to IMVs (100 μg of membrane protein) containing wild-type SecYEG or mutant derivatives was examined in buffer B as indicated. Following incubation (5 min; 4°C), the reactions (50 μl) were adjusted to a final concentration of 1.6 M sucrose in buffer B, and the resulting 150 μl of samples were overlaid with three consecutive layers of 1.4, 1.2, 0.25 M sucrose solutions. Following centrifugation (90 min; 436 000 *g*, TLA120.2 rotor, Beckman Optima TLX120) fractions of 50 μl were carefully removed, analysed by SDS-PAGE and visualized by immunostaining with α-SecA antibody.

In vivo *complementation*

In vivo genetic complementation of the cryosensitive AF659 *secYcs* strain was tested at 20°C (Baba *et al*., 1990; Taura *et al*., 1994). AF659 was transformed with plasmids carrying *secY* or mutant derivatives. AF659 *secYcs* were cultured at 37°C until mid-log phase. Cells were serially diluted 10-fold with LB and 6 μl of each was spotted on LB agar plates, which were photographed after 12 h at 37°C and 72 h at 20°C.

Isothermal titration calorimetry

Isothermal titration calorimetry was used to measure changes in enthalpy (ΔH) and stoichiometries of soluble SecY peptides binding to SecA as described (Keramisanou *et al*., 2006) using a VP-ITC (Microcal) instrument and Origin 7.0 software. SecA was added to the cell at 80 μM and peptides were contained in the injection syringe at 1 mM and added in 20 μl increments.

Protein translocation

Protein translocation was studied *in vitro* using proOmpA as a model protein as described (Karamanou *et al*., 1999). *In vivo* secretion was carried out using alkaline phosphatase as described (Derman *et al*., 1993; Osborne and Rapoport, 2007).

Chemicals/biochemicals

Nucleotides were from Roche; DNA enzymes were from Minotech; oligonucleotides were from the IMBB genomics facility; dNTPs were from Promega. [^{35}S]-Methionine (1000 Ci mmol^{-1}) and chromatography materials (except Ni^{2+} affinity; Qiagen) were from Amersham. Proteins were purified as described (van der Does *et al*., 1998; Karamanou *et al*., 1999). Soluble SecY peptides were synthesized by Alta Bioscience (Birmigham), dissolved in DMSO (100%) and stored at –20°C.

Acknowledgements

We are grateful to: D. Boyd (Beckwith Laboratory), S. Schulman (Rapoport Laboratory), V. Koronakis, A. Driessen and A. Flower for strains, plasmids and advice; G. Sianidis and M. Koukaki for genetic constructs, K. Tokatlidis and C. Lemoet for advice on peptide arrays; I. Gelis for structure modelling; G. Gouridis for useful discussions. Our research was supported by grants from the European Union (QLK3-CT-2000-00082 and LSHC-CT-2006-037834; to A.E.), the Greek General Secretariat of Research and the European Regional Development Fund (01AKMON46 and PENED03ED623; to A.E.) and by US National Institutes of Health Grant GM-73854 (to C.G.K.).

References

Baba, T., Jacq, A., Brickman, E., Beckwith, J., Taura, T., Ueguchi, C., *et al*. (1990) Characterization of cold-sensitive *secY* mutants of *Escherichia coli*. *J Bacteriol* **172:** 7005–7010.

Beck, K., Wu, L.F., Brunner, J., and Muller, M. (2000) Discrimination between SRP- and SecA/SecB-dependent substrates involves selective recognition of nascent chains by SRP and trigger factor. *EMBO J* **19:** 134–143.

Bessonneau, P., Besson, V., Collinson, I., and Duong, F. (2002) The SecYEG preprotein translocation channel is a conformationally dynamic and dimeric structure. *EMBO J* **21:** 995–1003.

den Blaauwen, T., Fekkes, P., de Wit, J.G., Kuiper, W., and Driessen, A.J. (1996) Domain interactions of the peripheral preprotein translocase subunit SecA. *Biochemistry* **35:** 11994–12004.

den Blaauwen, T., de Wit, J.G., Gosker, H., van der Does, C., Breukink, E.J., de Leij, L., and Driessen, A.J. (1997a) Inhibition of preprotein translocation and reversion of the membrane inserted state of SecA by a carboxyl terminus binding mAb. *Biochemistry* **36:** 9159–9168.

den Blaauwen, T., Terpetschnig, E., Lakowicz, J.R., and Driessen, A.J. (1997b) Interaction of SecB with soluble SecA. *FEBS Lett* **416:** 35–38.

Breukink, E., Nouwen, N., van Raalte, A., Mizushima, S., Tommassen, J., and de Kruijff, B. (1995) The C terminus of SecA is involved in both lipid binding and SecB binding. *J Biol Chem* **270:** 7902–7907.

Breyton, C., Haase, W., Rapoport, T.A., Kuhlbrandt, W., and Collinson, I. (2002) Three-dimensional structure of the bacterial protein-translocation complex SecYEG. *Nature* **418:** 662–665.

Brundage, L., Hendrick, J.P., Schiebel, E., Driessen, A.J., and Wickner, W. (1990) The purified *E. coli* integral membrane protein SecY/E is sufficient for reconstitution of SecA-dependent precursor protein translocation. *Cell* **62:** 649–657.

Chen, X., Xu, H., and Tai, P.C. (1996) A significant fraction of functional SecA is permanently embedded in the membrane. SecA cycling on and off the membrane is not

essential during protein translocation. *J Biol Chem* **271:** 29698–29706.
Chiba, K., Mori, H., and Ito, K. (2002) Roles of the C-terminal end of SecY in protein translocation and viability of *Escherichia coli*. *J Bacteriol* **184:** 2243–2250.
Dapic, V., and Oliver, D. (2000) Distinct membrane binding properties of N- and C-terminal domains of *Escherichia coli* SecA ATPase. *J Biol Chem* **275:** 25000–25007.
Derman, A.I., Puziss, J.W., Bassford, P.J., Jr, and Beckwith, J. (1993) A signal sequence is not required for protein export in prlA mutants of *Escherichia coli*. *EMBO J* **12:** 879–888.
van der Does, C., den Blaauwen, T., de Wit, J.G., Manting, E.H., Groot, N.A., Fekkes, P., and Driessen, A.J. (1996) SecA is an intrinsic subunit of the *Escherichia coli* preprotein translocase and exposes its carboxyl terminus to the periplasm. *Mol Microbiol* **22:** 619–629.
van der Does, C., Manting, E.H., Kaufmann, A., Lutz, M., and Driessen, A.J. (1998) Interaction between SecA and SecYEG in micellar solution and formation of the membrane-inserted state. *Biochemistry* **37:** 201–210.
Duong, F. (2003) Binding, activation and dissociation of the dimeric SecA ATPase at the dimeric SecYEG translocase. *EMBO J* **22:** 4375–4384.
Economou, A., and Wickner, W. (1994) SecA promotes preprotein translocation by undergoing ATP-driven cycles of membrane insertion and deinsertion. *Cell* **78:** 835–843.
Economou, A., Pogliano, J.A., Beckwith, J., Oliver, D.B., and Wickner, W. (1995) SecA membrane cycling at SecYEG is driven by distinct ATP binding and hydrolysis events and is regulated by SecD and SecF. *Cell* **83:** 1171–1181.
Eichler, J., and Wickner, W. (1997) Both an N-terminal 65-kDa domain and a C-terminal 30-kDa domain of SecA cycle into the membrane at SecYEG during translocation. *Proc Natl Acad Sci USA* **94:** 5574–5581.
Eichler, J., and Wickner, W. (1998) The SecA subunit of *Escherichia coli* preprotein translocase is exposed to the periplasm. *J Bacteriol* **180:** 5776–5779.
Eichler, J., Brunner, J., and Wickner, W. (1997) The protease-protected 30 kDa domain of SecA is largely inaccessible to the membrane lipid phase. *EMBO J* **16:** 2188–2196.
Gelis, I., Bonvin, A.M., Keramisanou, D., Koukaki, M., Gouridis, G., Karamanou, S., *et al.* (2007) Structural basis for signal-sequence recognition by the translocase motor SecA as determined by NMR. *Cell* **131:** 756–769.
Hartl, F.U., Lecker, S., Schiebel, E., Hendrick, J.P., and Wickner, W. (1990) The binding cascade of SecB to SecA to SecY/E mediates preprotein targeting to the *E. coli* plasma membrane. *Cell* **63:** 269–279.
Hunt, J.F., Weinkauf, S., Henry, L., Fak, J.J., McNicholas, P., Oliver, D.B., and Deisenhofer, J. (2002) Nucleotide control of interdomain interactions in the conformational reaction cycle of SecA. *Science* **297:** 2018–2026.
Jilaveanu, L.B., Zito, C.R., and Oliver, D. (2005) Dimeric SecA is essential for protein translocation. *Proc Natl Acad Sci USA* **102:** 7511–7516.
Joly, J.C., and Wickner, W. (1993) The SecA and SecY subunits of translocase are the nearest neighbors of a translocating preprotein, shielding it from phospholipids. *EMBO J* **12:** 255–263.
Karamanou, S., Vrontou, E., Sianidis, G., Baud, C., Roos, T., Kuhn, A., *et al.* (1999) A molecular switch in SecA protein couples ATP hydrolysis to protein translocation. *Mol Microbiol* **34:** 1133–1145.
Karamanou, S., Sianidis, G., Gouridis, G., Pozidis, C., Papanikolau, Y., Papanikou, E., and Economou, A. (2005) *Escherichia coli* SecA truncated at its termini is functional and dimeric. *FEBS Lett* **579:** 1267–1271.
Karamanou, S., Gouridis, G., Papanikou, E., Sianidis, G., Gelis, I., Keramisanou, D., *et al.* (2007) Preprotein-controlled catalysis in the helicase motor of SecA. *EMBO J* **26:** 2904–2914.
Keramisanou, D., Biris, N., Gelis, I., Sianidis, G., Karamanou, S., Economou, A., and Kalodimos, C.G. (2006) Disorder–order folding transitions underlie catalysis in the helicase motor of SecA. *Nat Struct Mol Biol* **13:** 594–602.
de Keyzer, J., van der Sluis, E.O., Spelbrink, R.E., Nijstad, N., de Kruijff, B., Nouwen, N., *et al.* (2005) Covalently dimerized SecA is functional in protein translocation. *J Biol Chem* **280:** 35255–35260.
Kim, Y.J., Rajapandi, T., and Oliver, D. (1994) SecA protein is exposed to the periplasmic surface of the *E. coli* inner membrane in its active state. *Cell* **78:** 845–853.
Manting, E.H., Kaufmann, A., van der Does, C., and Driessen, A.J. (1999) A single amino acid substitution in SecY stabilizes the interaction with SecA. *J Biol Chem* **274:** 23868–23874.
Manting, E.H., van Der Does, C., Remigy, H., Engel, A., and Driessen, A.J. (2000) SecYEG assembles into a tetramer to form the active protein translocation channel. *EMBO J* **19:** 852–861.
Matsumoto, G., Yoshihisa, T., and Ito, K. (1997) SecY and SecA interact to allow SecA insertion and protein translocation across the *Escherichia coli* plasma membrane. *EMBO J* **16:** 6384–6393.
Matsumoto, G., Nakatogawa, H., Mori, H., and Ito, K. (2000) Genetic dissection of SecA: suppressor mutations against the secY205 translocase defect. *Genes Cells* **5:** 991–999.
Mitra, K., Schaffitzel, C., Shaikh, T., Tama, F., Jenni, S., Brooks, C.L., *et al.* (2005) Structure of the *E. coli* protein-conducting channel bound to a translating ribosome. *Nature* **438:** 318–324.
Mori, H., and Ito, K. (2001) An essential amino acid residue in the protein translocation channel revealed by targeted random mutagenesis of SecY. *Proc Natl Acad Sci USA* **98:** 5128–5133.
Mori, H., and Ito, K. (2006) Different modes of SecY–SecA interactions revealed by site-directed *in vivo* photo-cross-linking. *Proc Natl Acad Sci USA* **103:** 16159–16164.
Natale, P., Swaving, J., van der Does, C., de Keyzer, J., and Driessen, A.J. (2004) Binding of SecA to the SecYEG complex accelerates the rate of nucleotide exchange on SecA. *J Biol Chem* **279:** 13769–13777.
Nishiyama, K., Suzuki, T., and Tokuda, H. (1996) Inversion of the membrane topology of SecG coupled with SecA-dependent preprotein translocation. *Cell* **85:** 71–81.
Or, E., Navon, A., and Rapoport, T. (2002) Dissociation of the dimeric SecA ATPase during protein translocation across the bacterial membrane. *EMBO J* **21:** 4470–4479.

Osborne, A.R., and Rapoport, T.A. (2007) Protein translocation is mediated by oligomers of the SecY complex with one SecY copy forming the channel. *Cell* **129:** 97–110.

Papanikou, E., Karamanou, S., Baud, C., Sianidis, G., Frank, M., and Economou, A. (2004) Helicase Motif III in SecA is essential for coupling preprotein binding to translocation ATPase. *EMBO Rep* **5:** 807–811.

Papanikou, E., Karamanou, S., Baud, C., Frank, M., Sianidis, G., Keramisanou, D., *et al.* (2005) Identification of the preprotein binding domain of SecA. *J Biol Chem* **280:** 43209–43217.

Papanikou, E., Karamanou, S., and Economou, A. (2007) Bacterial protein secretion through the translocase nanomachine. *Nat Rev Microbiol* **5:** 839–851.

Ramamurthy, V., and Oliver, D. (1997) Topology of the integral membrane form of *Escherichia coli* SecA protein reveals multiple periplasmically exposed regions and modulation by ATP binding. *J Biol Chem* **272:** 23239–23246.

Randall, L.L., Crane, J.M., Lilly, A.A., Liu, G., Mao, C., Patel, C.N., and Hardy, S.J. (2005) Asymmetric binding between SecA and SecB two symmetric proteins: implications for function in export. *J Mol Biol* **348:** 479–489.

Rapoport, T.A. (2007) Protein translocation across the eukaryotic endoplasmic reticulum and bacterial plasma membranes. *Nature* **450:** 663–669.

Reineke, U., Volkmer-Engert, R., and Schneider-Mergener, J. (2001) Applications of peptide arrays prepared by the SPOT-technology. *Curr Opin Biotechnol* **12:** 59–64.

Robson, A., Booth, A.E., Gold, V.A., Clarke, A.R., and Collinson, I. (2007) A large conformational change couples the ATP binding site of SecA to the SecY protein channel. *J Mol Biol* **374:** 965–976.

Scheuring, J., Braun, N., Nothdurft, L., Stumpf, M., Veenendaal, A.K., Kol, S., *et al.* (2005) The oligomeric distribution of SecYEG is altered by SecA and translocation ligands. *J Mol Biol* **354:** 258–271.

Schiebel, E., Driessen, A.J., Hartl, F.U., and Wickner, W. (1991) Delta mu H+ and ATP function at different steps of the catalytic cycle of preprotein translocase. *Cell* **64:** 927–939.

Schmidt, M., Dina, H., Ramamurthy, V., Mukerji, I., and Oliver, D. (2000) Nucleotide binding activity of SecA homodimer is conformationally regulated by temperature and altered by prlD and azi mutations. *J Biol Chem* **275:** 15540–15448.

Sianidis, G., Karamanou, S., Vrontou, E., Boulias, K., Repanas, K., Kyrpides, N., *et al.* (2001) Cross-talk between catalytic and regulatory elements in a DEAD motor domain is essential for SecA function. *EMBO J* **20:** 961–970.

van der Sluis, E.O., Nouwen, N., Koch, J., de Keyzer, J., van der Does, C., Tampe, R., and Driessen, A.J. (2006) Identification of two interaction sites in SecY that are important for the functional interaction with SecA. *J Mol Biol* **361:** 839–849.

Smith, M.A., Clemons, W.M., Jr, DeMars, C.J., and Flower, A.M. (2005) Modeling the effects of prl mutations on the *Escherichia coli* SecY complex. *J Bacteriol* **187:** 6454–6465.

Song, M., and Kim, H. (1997) Stability and solvent accessibility of SecA protein of *Escherichia coli*. *J Biochem (Tokyo)* **122:** 1010–1018.

Tam, P.C., Maillard, A.P., Chan, K.K., and Duong, F. (2005) Investigating the SecY plug movement at the SecYEG translocation channel. *EMBO J* **24:** 3380–3388.

Taura, T., Akiyama, Y., and Ito, K. (1994) Genetic analysis of SecY: additional export-defective mutations and factors affecting their phenotypes. *Mol Gen Genet* **243:** 261–269.

Tziatzios, C., Schubert, D., Lotz, M., Gundogan, D., Betz, H., Schagger, H., *et al.* (2004) The bacterial protein-translocation complex: SecYEG dimers associate with one or two SecA molecules. *J Mol Biol* **340:** 513–524.

Van den Berg, B., Clemons, W.M., Jr, Collinson, I., Modis, Y., Hartmann, E., Harrison, S.C., and Rapoport, T.A. (2004) X-ray structure of a protein-conducting channel. *Nature* **427:** 36–44.

van Voorst, F., van der Does, C., Brunner, J., Driessen, A.J., and de Kruijff, B. (1998) Translocase-bound SecA is largely shielded from the phospholipid acyl chains. *Biochemistry* **37:** 12261–12268.

Vrontou, E., Karamanou, S., Baud, C., Sianidis, G., and Economou, A. (2004) Global co-ordination of protein translocation by the SecA IRA1 switch. *J Biol Chem* **279:** 22490–22497.

van der Wolk, J.P., Fekkes, P., Boorsma, A., Huie, J.L., Silhavy, T.J., and Driessen, A.J. (1998) PrlA4 prevents the rejection of signal sequence defective preproteins by stabilizing the SecA–SecY interaction during the initiation of translocation. *EMBO J* **17:** 3631–3639.

Yahr, T.L., and Wickner, W.T. (2000) Evaluating the oligomeric state of SecYEG in preprotein translocase. *EMBO J* **19:** 4393–4401.

Supporting information

Additional supporting materials may be found in the online version of this article.

Please note: Blackwell Publishing are not responsible for the content or functionality of any supporting materials supplied by the authors. Any queries (other than missing material) should be directed to the corresponding author for the article.

